AJNR

CT-generated porous hydroxyapatite orbital floor prosthesis as a prototype bioimplant.

R A Levy, T M Chu, J W Halloran, S E Feinberg and S Hollister

AJNR Am J Neuroradiol 1997, 18 (8) 1522-1525
http://www.ajnr.org/content/18/8/1522

CT-Generated Porous Hydroxyapatite Orbital Floor Prosthesis as a Prototype Bioimplant

Richard A. Levy, Tien-Min G. Chu, John W. Halloran, Stephen E. Feinberg, and Scott Hollister

Summary: Hydroxyapatite bioceramic was used for the manufacture of an orbital floor prosthesis from spiral CT data acquired transaxially at 1-mm beam collimation, pitch of 1, and 0.2-mm reconstruction intervals. CT data were converted to vector file format for subsequent prosthesis manufacture on a stereolithography machine. The orbital floor prosthesis was engrafted onto an acrylic model of the orbit as a qualitative indication of its overall accuracy. High anatomic accuracy was achieved, as determined by visual inspection. Cross-hatching of the vector file data allowed a porous internal architecture of the prosthesis. Refinements in chemical structure of the hydroxyapatite bioceramic are expected to enhance mechanical properties.

Index terms: Eyes, surgery; Orbits, computed tomography

As the science of synthetic biomaterials matures from its present infancy, the role of the radiologist in the implementation of imaging-derived bioceramic prostheses for surgical applications will become more obvious. Among these applications is the creation of biodegradable scaffolds that induce ingrowth of bioengineered tissue in promoting accelerated postoperative healing (1). Such scaffolds will ideally be porous, resorbable, flexible, and workable while providing an anatomically accurate "carrier." The theoretical basis for such implants stands in contrast to some alloplastic materials that are bioinert and that heal by fibrous encapsulation rather than biointegration (2). The capacity for biointegration and remodeling allows a more physiological result.

The same factors that contribute to the accuracy of three-dimensional images reconstructed from medical imaging data will be critical in generating biomedical implants. These have been thoroughly reviewed, and include section thickness, threshold value, imaging plane, and reconstruction algorithm (3).

A new set of variables is introduced by the need to render the bioimplant integratable into surrounding tissue. Of these variables, implant pore size and pore directionality have been identified (4). Our purpose in this article is to illustrate the manufacture of an orbital floor prosthesis from a hydroxyapatite bioceramic by using medical imaging data. Points of potential user interactivity are emphasized.

Materials and Methods

A pediatric skull phantom was scanned in a water bath transaxially in a GE 9800 Hi-Speed spiral scanner (Milwaukee, Wis) using 1-mm beam collimation, pitch of 1, 0.2-mm section reconstruction intervals, 512 × 512 imaging matrix, 9.6-cm display field of view, 120 kVp, 200 mA, and a standard reconstruction algorithm. A threshold of 170 Hounsfield units was selected for 3-D model manufacture. Computed tomographic (CT) data were converted into a vectorized section format using a Silicon Graphics Indy workstation (Mountain View, Calif) for final model manufacture on a 3-D Systems 250 Model stereolithography machine (Valencia, Calif). This technology uses a laser beam to photopolymerize liquid into solid objects, layer by layer, on the basis of a file derived from medical imaging data. This file is generated from an operator-selected threshold value corresponding to the Hounsfield unit density of the target tissue. Subsequent to this binarization of the medical imaging data, a contour is automatically drawn around the target tissue, (CT) section by section, in vector file format. The internal component of the target region bounded by the contour map is then traversed by adjacent line segments that determine the laser trajectory as it photopolymerizes polymer or bioceramic.

A hydroxyapatite bioceramic was used to manufacture the model. The bioceramic is a suspension of hydroxyap-

Received July 10, 1996; accepted after revision November 13.

From the Department of Radiology, Neuroradiology Division (R.A.L.), the School of Dentistry (T-M.G.C.), the Department of Materials Science and Engineering, College of Engineering (T-M.G.C., J.W.H.), the Department of Oral Medicine, Pathology and Maxillofacial Surgery (S.E.F.), and the Orthopedics Research Lab (S.H.), University of Michigan Hospitals, Ann Arbor.

Address reprint requests to Richard A. Levy, MD, 4310 Woodview E, Saginaw, MI 48603.

AJNR 18:1522–1525, Sep 1997 0195-6108/97/1808–1522

atite powder in resin. The laser cures only the resin, so that when the resin is subsequently removed by heating in a furnace, a porous hydroxyapatite prosthesis remains. The pore size thus created ranges from tenths to several microns.

The 3-D modeling software enables the use of a crosshatch pattern to further render the internal portion of the implant porous. The width of the crosshatch cured by the laser is roughly 250 μm, with the spacing between crosshatches specified by the operator, ranging from several hundred microns to centimeters. The resin within the spaces defined by the crosshatches is not cured by the laser and can be drained away, creating porosity within the implant. A pore size of 2.18 mm was used in this experiment.

Before using the bioceramic, we generated a 3-D acrylic polymer model of the orbits, followed by a hydroxyapatite implant of the left orbital floor. The smaller region of interest used to build the left orbital floor implant was determined after vector file generation at the 3-D modeling workstation. The vector file containing both orbits was simply bisected, the right orbital data discarded, and only the data encompassing the left orbital floor used for implant manufacture. The original acrylic resin model was then softened in water, and the left orbital floor removed to allow implantation of the hydroxyapatite orbital floor prosthesis.

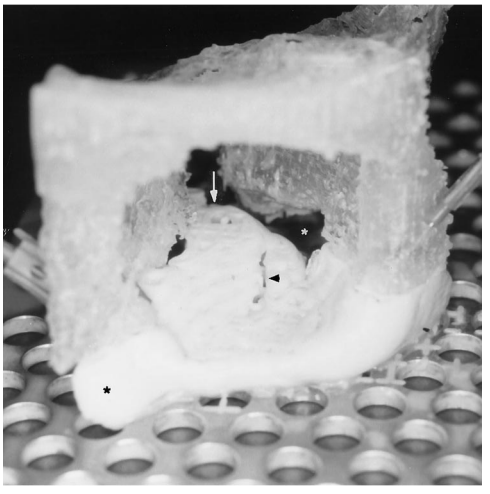

Fig 1. Hydroxyapatite orbital floor implant (*black asterisk*) engrafted onto an acrylic polymer model of the left orbit. *Arrow* shows internal cross-hatching of the posterior portion of the implant; *arrowhead* indicates infraorbital groove; *white asterisk* indicates inferior orbital fissure.

Discussion

A cosmetically acceptable appearance of the bioceramic orbital floor was achieved (Fig 1). The anatomic accuracy afforded by the stereolithography modeling process, in conjunction with the hydroxyapatite bioceramic, served as a prototype demonstration of implant manufacture for other biomaterials. Hydroxyapatite materials, while biocompatible and osteoconductive, are slow to biodegrade (5). Achieving a highly porous internal architecture may be a means of circumventing this problem. Development of more resorbable biomaterials is ongoing.

The ability to generate accurate anatomic models from volumetric CT data using stereolithography is well documented (6). A subtlety of the modeling process likely to receive considerable attention in the future is the engineering of pore size and pore directionality in the implant (Fig 2). Investigators have demonstrated superior osteoinduction in an animal model with implant porosity oriented across (rather than parallel to) calvarial defects (4). Our varying internal cross-hatching was only one option available to control implant porosity. Alternatively, only the target tissue contours for each CT section could have been used in the final data set for model production without internal cross-hatching or tissue "fill-in." Thus, after the operator-selected threshold is determined, the medical imaging data binarized, and the contour of the target tissue converted into vector file format, only this contour is photopolymerized. Such crude engineering was, in fact, used to make the acrylic polymer orbital model before the hydroxyapatite orbital floor prosthesis was manufactured. This contour-map construction contributed to the compressibility of the acrylic model when placed in water (Fig 3).

The vector file format into which medical imaging data are converted represents the industry standard. This vector file format creates a linear laser beam trajectory, but only after the contour of target tissue in the CT section has been traced by the laser. The laser beam follows adjacent line segments in the region to be photopolymerized, bounded by the contour map. The calibration of the stereolithography unit is such that discrete points along these line segments cannot be interactively modified, as is the case with other formats (such as rasterized toggle-point) no longer in use (7; and personal communication, Chris Manners, 3D Systems). It is at this stage, however, that cross-hatching can be engineered into the model or implant as a means of creating a porous internal architecture. It remains to be seen if implant porosity can be engineered interactively using simple

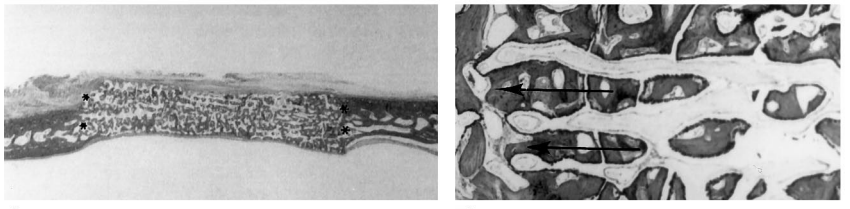

A B

Fig 2. Osteoinduction in a hydroxyapatite graft with pores running longitudinally across a calvarial defect. More osteoinduction occurs than when the pores are oriented parallel to the margins of the calvarial defect. *Arrows* show the pores replaced by ingrown bone; *asterisks* show graft/calvarial interfaces (from Magan and Ripamonti [4]).

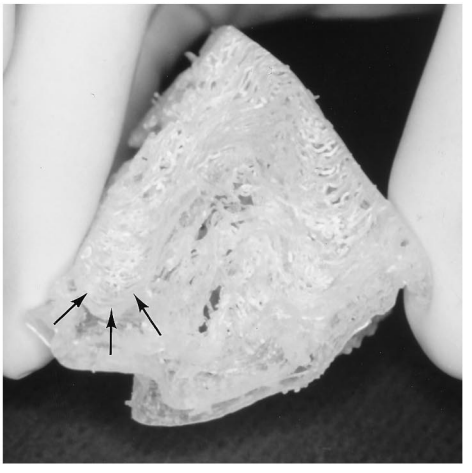

Fig 3. After the acrylic polymer model of the left orbit is placed in water, it becomes compressible. Photograph shows "intracranial" view of the orbital roof after immersion in water. Note buckling of layered contours in the model during compression (*arrows*), demonstrating that internal architecture plays a role in the physical properties of the model.

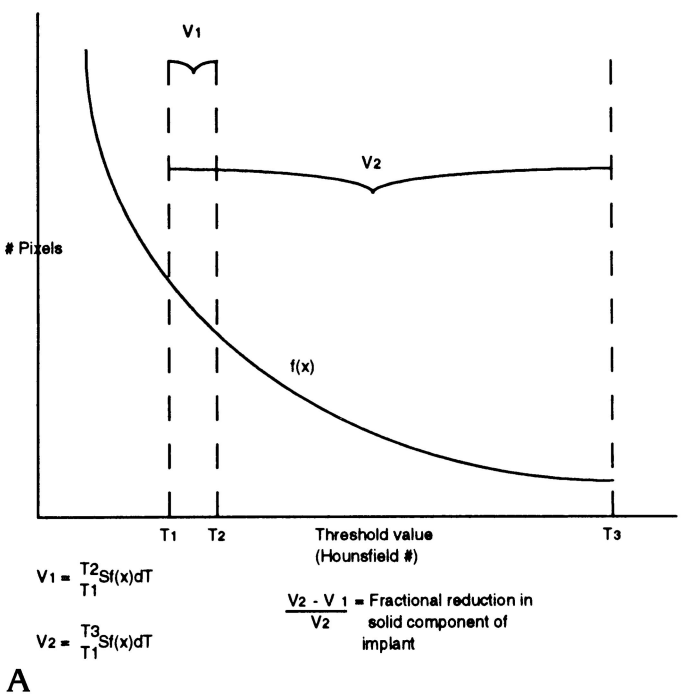

A

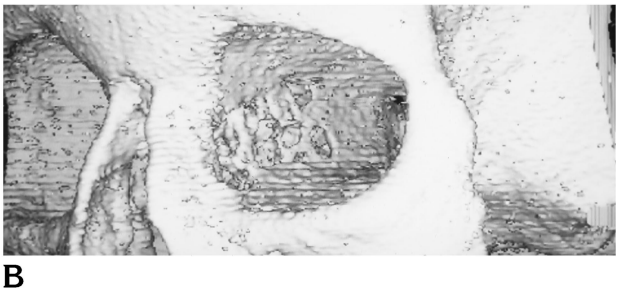

B

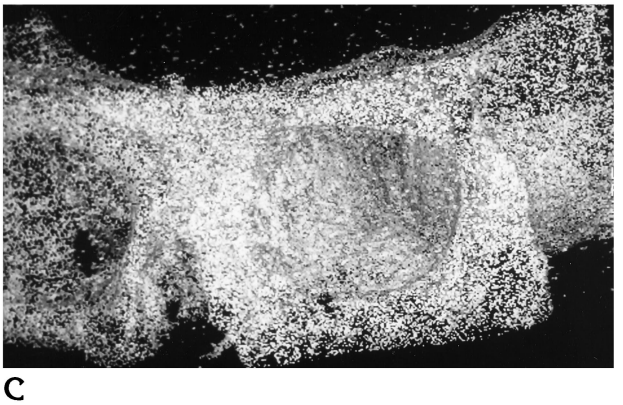

C

Fig 4. Idealized histogram of CT data of a skull scanned in a water bath (*A*). T1 is the threshold at which background water pixels start to appear and corresponds to 3-D image in *B*. Instead of using an "infinite" upper threshold, T3, an upper threshold, T2, very close numerically to T1, allows creation of a porous data set for implant manufacture (*C*). This algorithm takes advantage of partial volume averaging at the skull/water interface to produce a porous 3-D imaging data set. (*B* and *C* were reconstructed from the CT data set in Figures 1 and 3.)

thresholding steps at the 3-D imaging workstation before the vector file data set for stereolithography is generated. An algorithm that takes advantage of partial volume averaging at high-contrast interfaces and that causes significant changes in porosity over narrow threshold ranges is currently under investigation (Fig 4).

Acknowledgments

We thank Jane B. Mitchell for preparing the manuscript, Bob Combs for photography, Mark Bliek of Materialize for his time and use of imaging software, and Tom Chenevert and Frank Londy for technical assistance.

References

1. Kucan JO, Lee RC. Plastic surgery. *JAMA* 1996;275:1844–1845
2. Dougherty WR, Wellisz T. The natural history of alloplastic implants in orbital floor reconstruction: an animal model. *J Craniofac Surg* 1994;5:26–32
3. Levy RA. Three-dimensional craniocervical helical CT: is isotropic imaging possible? *Radiology* 1995;197:645–648
4. Magan A, Ripamonti U. Geometry of porous hydroxyapatite implants influences osteogenesis in baboons. *J Craniofac Surg* 1996; 7:71–78
5. Bucholz RW, Buckwalter JA. Orthopedic surgery. *JAMA* 1996; 1836–1837
6. Ono I, Gunji H, Suda K, Kaneko F. Method for preparing an exact-size model using helical volume scan computed tomography. *Plast Reconstruct Surg* 1994;1363–1371
7. Levy RA, Guduri S, Crawford RH. Preliminary experience with selective laser sintering models of the human temporal bone. *AJNR Am J Neuroradiol* 1994;15:473–477